Journal of Inorganic Biochemistry 220 (2021) 111372

Contents lists available at ScienceDirect

Journal of Inorganic Biochemistry

journal homepage: www.elsevier.com/locate/jinorgbio

Effect of the replacement of tripodal 4N donors by two 2N chelators on the redox and cytotoxic activity of maltolato and deferipronato containing Co(III) complexes

Sándor Nagy [a], Emese Tóth [b], István Kacsir [a], Attila Makai [a], Attila Csaba Bényei [c], Péter Buglyó [a,*]

[a] Department of Inorganic and Analytical Chemistry, University of Debrecen, H-4032 Debrecen, Egyetem tér 1, Hungary
[b] Department of Medical Chemistry, University of Debrecen, H-4032 Debrecen, Egyetem tér 1, Hungary
[c] Department of Physical Chemistry, University of Debrecen, H-4032 Debrecen, Egyetem tér 1, Hungary

ARTICLE INFO

Keywords:
Co^{III} complexes
DHP
Redox behaviour
Anticancer
X-ray structures
1,10-phenantroline

ABSTRACT

Fourteen novel Co^{III} ternary complexes with the general formula $[Co(4N)(2O)]X_2$ or $[Co(2N)_2(2O)]X_2$ where 4N = tris(2-aminoethyl)amine (tren) or tris(2-pyridylmethyl)amine (tpa); 2N = 1,10-phenantroline (phen), 2,2′-bipyridine (bipy), 1,2-diaminoethane (en) or 2-(aminomethyl)pyridine (ampy) and 2O = 1,2-dimethyl-3-hydroxy-4(1*H*)-pyridinone (dhpH), 3-hydroxy-2-methyl-4-pyrone (maltH) or 2-ethyl-3-hydroxy-4*H*-pyran-4-one (etmaltH) were synthesized, characterized and their redox features explored. Molecular structure of some selected $[Co(2N)_2(2O)](ClO_4)_2$ (2N = phen, bipy, en; 2O = dhp, malt) or $[Co(4N)(2O)](ClO_4)_2$ (4N = tpa; 2O = etmalt) type complexes were assessed by X-ray diffraction and showed the expected octahedral geometry. Replacement of the 4N donor ligands by two 2N donor ligands resulted in the decrease of the cathodic peak potential of the complexes indicating easier reduction and allowing therefore the tailoring of the redox properties of the complexes. Screening of selected compounds against a human derived cancer cell line, HeLa, showed that, unlike the $[Co(4N)(2O)]X_2$ derivatives, the complexes containing 2N = bipy or phen ligands have better anticancer activity than cisplatin or carboplatin.

1. Introduction

Selectivity is a key issue to obtain more suitable metal based drugs with fewer side effects that are potent even at low concentrations. To combat cancer the differences between the properties of healthy and cancer cells/tissues need to be considered. Among them hypoxia in cancer tissues means a more reductive environment allowing the selective reduction of prodrugs that carry molecules with anticancer potential. Remarkable candidates can be the octahedral, inert cobalt(III) complexes with tailored redox properties capable of selective reduction under hypoxic conditions that results in the intracellular formation of labile and less stable cobalt(II) complexes [1–5]. Upon dissociation of the Co(II) species formed the drug molecule can be released and act at the site of the tumour. It was also demonstrated that the Co(II) formed in situ upon reduction of the Co(III) prodrugs can generate reactive oxygen species (ROS) and causes mitochondrial DNA damage and subsequent apoptosis [6,7]. It should also be emphasized that the tailored redox behaviour of these Co(III) complexes alone is not sufficient; among others, the proper ligand exchange and reduction rates of the chaperon Co(III) complexes are also of high importance.

Previously it was shown that octahedral Co(III) complexes with a 4N + 2O donor atom arrangement have suitable reduction potential values being in the range of −200 to −400 mV characteristic for hypoxic conditions [3,8–12]. While $[Co(6N)]^{3+}$ type species would be too hard to reduce, increasing number of O donors in the coordination sphere would result in the stabilization of the +2 oxidation state of the metal ion in the complexes. Our detailed, recent studies also highlighted that, depending upon the type of the N donor and the size of the chelates that are formed with Co(III) when a tripodal 4N donor amine is coordinating, the redox potential of the complexes can be tuned. In particular, study of the redox features of $[Co^{III}(4N)Cl_2]^+$ complexes incorporating symmetric or asymmetric tripodal amines with aliphatic and/or aromatic (pyridyl) N donors revealed that the replacement of an aliphatic 4N donor amine forming (5 + 6 + 6) joined chelates by tris(2-aminoethyl)

* Corresponding author.
E-mail address: buglyo@science.unideb.hu (P. Buglyó).

https://doi.org/10.1016/j.jinorgbio.2021.111372
Received 18 December 2020; Received in revised form 20 January 2021; Accepted 21 January 2021
Available online 28 January 2021

amine (tren) capable of forming (5 + 5 + 5) joined chelates resulted in ~330 mV less negative reduction potential for the latter complex. A further, up to ca. 500 mV, positive shift was observed by introducing two, and especially, three π-back-bonding pyridyl rings (in tris(2-pyridylmethyl)amine (tpa)) into the chains of the tetraamines [13]. Similar trends regarding the effect of the size of the chelate were previously also found for $[Co^{III}(4N)(O_2CO)]^{2+}$ type complexes (4N = tripodal trispyridyl tetramines capable of forming 5 + 5 + 5, 5 + 5 + 6, 5 + 6 + 6 or 6 + 6 + 6 fused chelates) revealing the easiest reduction of the complex with the 4N ligand that coordinates via a 6 + 6 + 6 fashion [14].

It was also demonstrated that with given 4N donor amine and 2O donor ligand the obtained $[Co(4N)(2O)]^{n+}$ type ternary complex can have too high thermodynamic stability as well, accompanied by very negative redox potential. For instance, in our previous study we have found this situation for some benzohydroxamato ($[Co(tren)(bha)](ClO_4)_2$; $E_{pc} = -571$ mV vs. H_2/H^+) and benzohydroxymato ($[Co(tren)(bhaH_{-1})]ClO_4$; $E_{pc} = -790$ mV vs. H_2/H^+ where bhaH = benzohydroxamic acid) complexes [13]. Replacement therefore the tripodal 4N donor by two 4N donor ligands may provide with an adequate platform for the synthesis of $[Co(2N)_2(2O)]^{n+}$ type ternary complexes with tailored redox features. A further advantage can be expected if the used 4N donors themselves have additional biological effects too. The selected 1,10-phenantroline (phen), together with its substituted derivatives, is well-known for its anticancer potential and metalloprotease inhibitory effect [15–18]. $[Co(2N)_2Cl_2]Cl$ (2N = phen, 2,2′-bipyridine (bipy), 1,2-diaminoethane (en)) complexes were also shown to bind DNA covalently retaining the structure of the helix [19]. Recently it was also demonstrated that $[Co(2N)_2(2O)]PF_6$ (4N = phen, bipy; 2O = salicylate derivative) type complexes are capable of releasing the 2O donor anti-inflammatory drug under reductive conditions and exhibited micromolar potency towards HMLER and HMLER-shEcad cells [20]. As for a 2O donor ligand in this study primarily 1,2-dimethyl-3-hydroxy-4(1*H*)-pyridinone (deferiprone, dhpH) was selected with a view of synthesizing complexes where the 2O donor ligand with strong iron sequestering capability can have an additional effect as anticancer agent via disturbing the elevated iron-uptake processes of the cancer cell. While it shows no or mild anticancer activity towards various cancer cell lines [21], dhpH is also served as a model compound in the way of developing novel ambidentate ligands in which beside the 2O donor chelating part based on dhpH, a further 2N donor metal binding unit can function to carry another metal ion with proven anticancer activity [22].

Herein we report on the synthesis, analytical characterization, solid state structure, redox properties and anticancer potential against a human derived cancer cell line, HeLa, of novel Co(III) complexes incorporating phen and dhp. In order to explore the effect of the 4N → 2x2N replacement on the redox properties of the ternary Co(III) complexes, tren and tpa while for the comparison of the effect of the various chelate sizes and type of the coordinating donor atoms, the appropriate 2N analogues of phen, bipy, en, and 2-(aminomethyl)pyridine (ampy) were also involved in the study. To gain a deeper insight into the effect of a weaker iron sequestering agent on the redox properties and anticancer effect of the complexes, 3-hydroxy-2-methyl-4-pyrone (maltol, maltH) as a dhp-related 2O donor chelating ligand and an FDA approved food additive, together with 2-ethyl-3-hydroxy-4*H*-pyran-4-one (ethyl maltol, etmaltH) was also used in the study (Fig. 1).

2. Experimental

2.1. Materials and reagents

$CoCl_2{\cdot}6H_2O$, $NaNO_2$, tren, phen, bipy, ampy, en, $NaClO_4{\cdot}H_2O$, maltH, etmaltH, Et_3N, methanol, ethanol, KOH, NaOH, KNO_3, DMSO, D_2O, d^6-DMSO, MTT, EMEM and PBS tablets were commercial products from Merck, Fluka, TCI, Sigma-Aldrich, Reanal and Euroiso-top. Tpa [23], dhpH [24], $[Co(tren)(NO_2)_2]Cl$, $[Co(tren)Cl_2]Cl$, $[Co(tpa)(NO_2)_2]Cl$, $[Co(tpa)Cl_2]Cl$ [25], $[Co(en)_2Cl_2]Cl$ [26], $[Co(phen)_2Cl_2]Cl$, $[Co(bipy)_2Cl_2]Cl$ [19], $[Co(ampy)_2(NO_2)_2]NO_3$, $[Co(ampy)_2Cl_2]Cl$ [27], were synthesized and purified according to literature procedures. Milli-Q ultrapure water was used as a solvent for the samples and stock solutions.

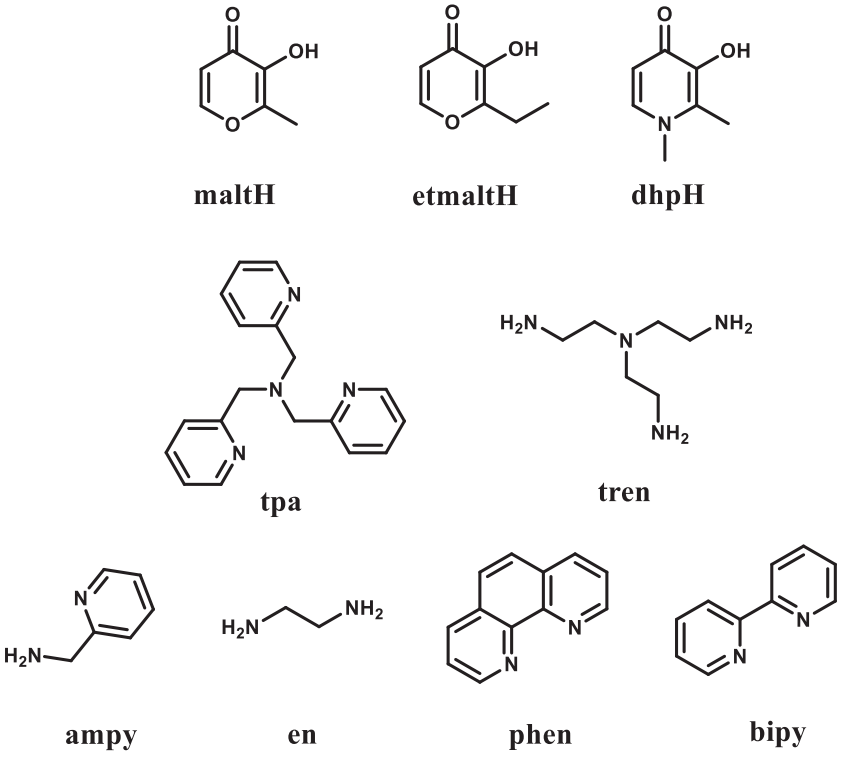

Fig. 1. Formulae and abbreviations of the ligands used in this study.

2.2. Syntheses

***CAUTION**: Although we never have experienced any problems, perchlorate salts are potentially explosive.*

$[Co(en)_2(malt)](ClO_4)_2$ (**1**)

MaltH (90 mg, 0.71 mmol) was suspended in 5 mL water and the suspension was added to the 5 mL water solution of $[Co(en)_2Cl_2]Cl$ (202 mg, 0.71 mmol). Finally, Et_3N (140 μL, 1.00 mmol) was added dropwise to the mixture. The red solution was stirred at 55 °C for 4 h and kept at room temperature overnight. $NaClO_4 \cdot H_2O$ (98 mg, 0.70 mmol) was added to the solution. The reaction mixture was nearly 3 mL evaporated, slowly red microcrystalline solid appeared. The solid was filtered off, washed with cool ethanol and dried in vacuo. Yield: 37 mg (10%). ^{1}H NMR (400 MHz, D_2O): δ/ppm = 8.09 (d, 1H, malt H); 6.90 (d, 1H, malt H); 2.91–2.66 (m, 8H, -CH_2); 2.49 (s, malt -CH_3). IR (KBr)/cm^{-1}: 3423, 3306, 3255, 3165, 1599, 1581, 1552, 1474, 1275, 1214, 1120, 1004, 930, 849, 826, 624, 583. Anal. Required for $CoC_{10}H_{21}N_4O_{11}Cl_2$: C, 23.87, H, 4.21, N, 11.14%. Found: C, 23.98, H, 4.22, N, 11.04%. MS (ESI, positive ion): *m/z* 303.0844 $[Co^{III}(en)_2(malt)\text{-}H]^+$ (simulated: 303.0862); 243.0159 $[Co^{III}(en)(malt)\text{-}2H]^+$ (simulated: 243.0174); 225.9895 $C_8H_9CoNO_3$ (simulated: 225.9909); 213.9894 $C_7H_9CoNO_3$ (simulated: 213.9909); 212.9818 $C_7H_7CoNO_3$ (simulated: 212.9831); 152.0459 $[Co(en)_2(malt)]^{2+}$ (simulated: 152.0467).

$[Co(phen)_2(malt)](ClO_4)_2$ (**2**)

MaltH (29 mg, 0.23 mmol) dissolved in 4 mL methanol and Et_3N (29 μL, 0.21 mmol) was added to the 3 mL methanol suspension of $[Co(phen)_2Cl_2]Cl$ (116 mg, 0.22 mmol). The suspension was stirred at 55 °C for 4 h. The mixture became clear and the colour of the reaction mixture turned into red. The mixture was standing at 4 °C overnight. $NaClO_4 \cdot H_2O$ (59 mg, 0.42 mmol) in 1 mL methanol was added to the solution. Red solid appeared immediately. The solid was filtered off, washed with cold MeOH and dried in vacuo. Yield: 89 mg (57%). ^{1}H NMR (400 MHz, d^6-DMSO): δ/ppm = 9.31 (d, 2H, Ar-H phen); 9.13 (d, 1H, Ar-H phen); 9.03–8.95 (m, 3H, Ar-H phen); 8.59 (d, 2H, Ar-H phen); 8.49 (d, 1H, malt H); 8.47–8.42 (m, 4H, Ar-H phen); 7.88–7.78 (m, 4H, Ar-H phen); 7.13 (d, 1H, malt H); 2.39 (s, 3H, malt -CH_3). IR (KBr)/cm^{-1}: 3428, 1605, 1546, 1522, 1471, 1430, 1270, 1209, 1148, 1090, 848, 717, 624, 586. Anal. Required for $CoC_{30}H_{21}N_4O_{11}Cl_2 \cdot H_2O$: C, 47.33, H, 3.04, N, 7.36%. Found: C, 47.52, H, 3.02, N, 7.50%. MS (ESI, positive ion): *m/z* 272.0452 $[Co^{III}(phen)_2(malt)]^{2+}$ (simulated: 272.0467). On standing X-ray quality crystals appeared from the mother liquor.

$[Co(phen)_2(etmalt)](ClO_4)_2$ (**3**)

This was synthesized as **2** using $[Co(phen)_2Cl_2]Cl$ (100 mg, 0.19 mmol), etmaltH (30 mg, 0.21 mmol), Et_3N (32 μL, 0.23 mmol) and $NaClO_4 \cdot H_2O$ (56 mg, 0.40 mmol). The product was isolated as a microcrystalline purple/red solid. Yield: 40 mg (28%). ^{1}H NMR (400 MHz, d^6-DMSO): δ/ppm = 9.32 (d, 2H, Ar-H phen); 9.09 (d, 1H, Ar-H phen); 9.02–8.95 (m, 3H, Ar-H phen); 8.59 (dd, 2H, Ar-H phen); 8.52 (d, 1H, etmalt H); 8.50–8.41(m, 4H, Ar-H phen); 7.92 (d, 1H, Ar-H phen); 7.86–7.78 (m, 3H, Ar-H phen); 7.14 (d, 1H, etmalt H); 2.74 (m, 2H, etmalt -CH_2); 1.00 (t, 3H, etmalt -CH_3). IR (KBr)/cm^{-1}: 3432, 1597, 1543, 1522, 1472, 1430, 1092, 846, 717, 623. Anal. Required for $C_{31}H_{23}Cl_2CoN_4O_{11} \cdot H_2O$: C, 48.02, H, 3.25, N, 7.23%. Found: C, 47.75, H, 3.26, N, 7.26%. MS (ESI, positive ion): *m/z* 279.0528 $[Co^{III}(phen)_2(etmalt)]^{2+}$ (simulated: 279.0546).

$[Co(phen)_2(dhp)](ClO_4)_2$ (**4**)

This was synthesized as **2** using $[Co(phen)_2Cl_2]Cl$ (100 mg, 0.19 mmol), dhpH (26 mg, 0.19 mmol), Et_3N (26 μL, 0.19 mmol) and $NaClO_4 \cdot H_2O$ (53 mg, 0.38 mmol). The reaction mixture was green and the product was isolated as a microcrystalline green solid. Yield: 75 mg (52%). ^{1}H NMR (400 MHz, d^6-DMSO): δ/ppm = 9.26 (d, 2H, Ar-H phen); 9.00 (d, 2H, Ar-H phen); 8.96 (d, 2H, Ar-H phen); 8.55 (d, 2H, Ar-H phen); 8.46 (d, 2H, Ar-H phen); 8.42–8.38 (m, 2H, Ar-H phen); 7.85–7.76 (m, 5H, Ar-H phen, dhp H); 6.78 (d, 1H, dhp H); 3.79 (s, 3H, dhp N-CH_3); 2.27 (s, 3H, dhp -CH_3). IR (KBr)/cm^{-1}: 3478, 3064, 1610, 1520, 1499, 1459, 1430, 1330, 1277, 1150, 1090, 1038, 849, 718, 623. Anal. Required for $CoC_{31}H_{24}Cl_2N_5O_{10} \cdot H_2O$: C, 48.08, H, 3.38, N, 9.04%. Found: C, 47.99, H, 3.50, N, 9.04%. MS (ESI, positive ion): *m/z* 278.5626 $[Co^{III}(phen)_2(dhp)]^{2+}$ (simulated: 278.5625); 209.5337 $[Co^{II}(phen)_2]^{2+}$ (simulated: 209.5348). On standing X-ray quality crystals appeared from the mother liquor.

$[Co(bipy)_2(malt)](ClO_4)_2$ (**5**)

100 mg (0.21 mmol) $[Co(bipy)_2Cl_2]Cl$ was suspended in 10 mL water. The suspension was stirred at 80 °C to get a clear solution. 31 mg (0.25 mmol) maltH and 8.75 mg (0.22 mmol) NaOH was added to the purple solution. The mixture was heated at reflux for 2 h and kept at 4 °C overnight. Purple solid appeared slowly by adding $NaClO_4 \cdot H_2O$ (31 mg, 0.22 mmol). The solid was filtered off and dried in vacuo. Yield: 19 mg (13%). ^{1}H NMR (400 MHz, d^6-DMSO): δ/ppm = 9.03 (d, 2H, Ar-H bipy); 8.94–8.89 (m, 2H, Ar-H bipy); 8.77 (d, 1H, Ar-H bipy); 8.67 (t, 2H, Ar-H bipy); 8.65 (d, 1H, Ar-H bipy); 8.47–8.40 (m, 3H, malt H and Ar-H bipy); 8.11–8.06 (m, 2H, Ar-H bipy); 7.70–7.56 (m, 4H, Ar-H bipy); 7.12 (d, 1H, malt H); 2.40 (s, 3H, malt -CH_3). IR (KBr)/cm^{-1}: 3421, 3078, 1606, 1542, 1500, 1468, 1451, 1357, 1315, 1268, 1215, 1167, 1092, 849, 768, 728, 623, 582. Anal. Required for $CoC_{26}H_{21}N_4O_{11}Cl_2$: C, 44.91, H, 3.04, N, 8.06%. Found: C, 44.76, H, 3.13, N, 8.09%. MS (ESI, positive ion): *m/z* 248.0455 $[Co^{III}(bipy)_2(malt)]^{2+}$ (simulated: 248.0467); 185.5342 $[Co^{II}(bipy)_2]^{2+}$ (simulated: 185.5348). On standing X-ray quality crystals appeared from the mother liquor.

$[Co(bipy)_2(etmalt)](ClO_4)_2$ (**6**)

It was synthesized analogously to **2** using $[Co(bipy)_2Cl_2]Cl$ (100 mg, 0.21 mmol), etmaltH (31 mg, 0.22 mmol), Et_3N (33 μL, 0.24 mmol) and $NaClO_4 \cdot H_2O$ (60 mg, 0.43 mmol). The product was isolated as a microcrystalline purple solid. Yield: 28 mg (19%). ^{1}H NMR (400 MHz, d^6-DMSO): δ/ppm = 9.04 (d, 1H, Ar-H bipy); 9.02 (d, 1H, Ar-H bipy); 8.94 (d, 1H, Ar-H bipy); 8.90 (d, 1H, Ar-H bipy); 8.74 (d, 1H, Ar-H bipy); 8.70–8.65 (m, 2H, Ar-H bipy); 8.62 (d, 1H, Ar-H bipy); 8.49 (d, 1H, etmalt H); 8.47–8.40 (m, 2H, Ar-H bipy); 8.12 (t, 1H, Ar-H bipy); 8.06 (t, 1H, Ar-H bipy); 7.77 (d, 1H, Ar-H bipy); 7.67 (t, 1H, Ar-H bipy); 7.61 (t, 1H, Ar-H bipy); 7.58 (t, 1H, Ar-H bipy); 7.12 (d, 1H, etmalt H); 2.40 (s, 3H, etmalt -CH_3); 2.76 (q, 2H, etmalt -CH_2); 1.02 (t, 3H, etmalt -CH_3). IR (KBr)/cm^{-1}: 3432, 3091, 1598, 1543, 1470, 1451, 1093, 770, 729, 623. Anal. Required for $C_{27}H_{23}Cl_2CoN_4O_{11} \cdot 0.5H_2O$: C, 45.14, H, 3.37, N, 7.80%. Found: C, 44.92, H, 3.40, N, 7.90%. MS (ESI, positive ion): *m/z* 255.0533 $[Co^{III}(bipy)_2(etmalt)]^{2+}$ (simulated: 255.0546); 185.5342 $[Co^{II}(bipy)_2]^{2+}$ (simulated: 185.5348).

$[Co(bipy)_2(dhp)](ClO_4)_2$ (**7**)

To the purple solution of $[Co(bipy)_2Cl_2]Cl$ (51 mg, 0.11 mmol) in 5 mL water was added dhpH (15 mg, 0.11 mmol) and NaOH (4.2 mg, 0.11 mmol). The mixture was refluxed overnight. The colour of the reaction mixture changed from red to green. Green solid appeared immediately by adding $NaClO_4 \cdot H_2O$ (15 mg, 0.11 mmol). The solid was filtered off and dried in vacuo. Yield: 56 mg (72%). ^{1}H NMR (400 MHz, d^6-DMSO): δ/ppm = 9.00 (d, 2H, Ar-H bipy); 8.90 (d, 2H, Ar-H bipy); 8.68–8.60 (m, 4H, Ar-H bipy); 8.41 (t, 2H, Ar-H bipy); 8.04 (t, 2H, Ar-H bipy); 7.75 (d, 1H, dhp H); 7.64–7.61 (m, 4H, Ar-H bipy); 6.76 (d, 1H, dhp H); 3.79 (s, 3H, dhp N-CH_3); 2.29 (s, 3H, dhp –CH_3). IR (KBr)/cm^{-1}: 3434, 3118, 3086, 1500, 1467, 1450, 1336, 1271, 1093, 769, 730, 623. Anal. Required for $C_{27}H_{24}Cl_2CoN_5O_{10} \cdot 0.5H_2O$: C, 45.21, H, 3.51, N, 9.76%. Found: C, 45.45, H, 3.64, N, 9.74%. MS (ESI, positive ion): *m/z* 254.5612 $[Co^{III}(bipy)_2(dhp)]^{2+}$ (simulated: 254.5625); 185.5343 ($[Co^{II}(bipy)_2]^{2+}$ (simulated: 185.5348).

$[Co(ampy)_2(malt)](ClO_4)_2$ (**8**)

MaltH (34 mg, 0.27 mmol) and NaOH (12.4 mg, 0.31 mmol) were dissolved in 10 mL water/MeOH mixture (1:1). $[Co(ampy)_2Cl_2]Cl$ (102 mg, 0.27 mmol) dissolved in 5 mL water was added and the mixture was stirred at 55 °C for 4 h. The mixture was kept at 4 °C overnight and $NaClO_4 \cdot H_2O$ (73 mg, 0.52 mmol) was added. The solution was evaporated and on cooling overnight at 4 °C the title compound appeared. The red solid was filtered off and dried in vacuo. Yield: 10 mg (6%). ^{1}H NMR (400 MHz, d^6-DMSO): δ/ppm = 8.39 (d, 2H, Ar-H ampy); 8.37 (d, 1H,

malt H); 8.21 (d, 1H, Ar-H ampy); 8.15 (t, 2H, Ar-H ampy); 7.76–7.65 (m, 4H, Ar-H ampy); 7.04 (d, 1H, malt H); 6.43 (m, 1H, ampy -NH_2); 6.19 (m, 1H, ampy -NH_2); 5.55 (m, 2H, ampy -NH_2); 4.35–4.15 (m, 4H, ampy -CH_2); 2.52 (s, 3H, malt -CH_3). IR (KBr)/cm^{-1}: 3435, 3249, 1603, 1550, 1474, 1120, 1109, 1091, 626. Anal. Required for $C_{18}H_{21}Cl_2CoN_4O_{11}$: C, 36.08, H, 3.53, N, 9.35%. Found: C, 36.47, H, 3.60, N, 9.27%. MS (ESI, positive ion): *m/z* 499.0424 [Co^{III}(ampy)$_2$(-malt)]ClO_4^+ (simulated: 499.0425).

[Co(tren)(malt)]$(ClO_4)_2$ (**9**)

[Co(tren)Cl_2]Cl·H_2O (401 mg, 1.22 mmol) and maltH (161 mg, 1.28 mmol) were solved in 10 mL water. 1.28 mL KOH (1 M) was added to the solution dropwise and the suspension was stirred at 70 °C for 5 h and overnight at room temperature. The red solution was evaporated to dryness and dissolved in 45 mL EtOH. After cooling and filtering to the solution $NaClO_4$·H_2O (342 mg, 2.44 mmol) in 4 mL EtOH was added. The red solid appeared immediately was filtered off and dried in vacuo. Yield: 458 mg (71%). ^{1}H NMR of isomer A (400 MHz, D_2O): δ/ppm = 8.17 (d, 1H, malt H); 7.00 (d, 1H, malt H); 3.68 (m, 2H, tren -CH_2); 3.43 (m, 2H, tren -CH_2); 3.21 (m, 4H, tren -CH_2); 2.98 (m, 4H, tren -CH_2); 2.52 (s, 3H, malt -CH_3). ^{1}H NMR of isomer B (400 MHz, D_2O): δ/ppm = 8.12 (d, 1H, malt H); 6.91 (d, 1H, malt H); 3.68 (m, 2H, tren -CH_2); 3.43 (m, 2H, tren -CH_2); 3.21 (m, 4H, tren -CH_2); 2.98 (m, 2H, tren -CH_2); 2.88 (m, 2H, tren -CH_2); 2.58 (s, 3H, malt –CH_3). Ratio of the Isomer A: Isomer B = 7: 1. IR (KBr)/cm^{-1}: 3421, 3285, 3207, 3120, 1611, 1552, 1473, 1273, 1206, 1092, 850, 826, 747, 624. Anal. Required for $C_{12}H_{23}Cl_2CoN_4O_{11}$: C, 27.24, H, 4.38, N, 10.59%. Found: C, 27.01, H, 4.44, N, 10.48%. MS (ESI, positive ion): *m/z* 304.0341 [Co^{II}(tren)]$(ClO_4)^+$ (simulated: 304.0343); 329.1016 [Co^{III}(tren)(malt)-H]$^+$ (simulated: 329.1018); 429.0581 [Co^{III}(tren)(malt)]$(ClO_4)^+$ (simulated: 429.0582).

[Co(tren)(etmalt)]$(ClO_4)_2$ (**10**)

It was synthesized analogously to **9** using [Co(tren)Cl_2]Cl·H_2O (203 mg, 0.62 mmol), etmaltH (90 mg, 0.64 mmol), NaOH (1 M, 0.64 mL) and $NaClO_4$·H_2O (170 mg, 1.20 mmol) dissolved in 3 mL EtOH/MeOH. The product was isolated as a microcrystalline purple solid. Yield: 142 mg (44%). ^{1}H NMR of isomer A (400 MHz, D_2O): δ/ppm = 8.19 (d, 1H, etmalt H); 7.00 (d, 1H, etmalt H); 3.80–2.80 (m, 14H, tren -CH_2; etmalt -CH_2); 1.26 (t, 3H, etmalt -CH_3). ^{1}H NMR of isomer B (400 MHz, D_2O): δ/ppm = 8.14 (d, 1H, etmalt H); 6.90 (d, 1H, etmalt H); 3.80–2.80 (m, 14H, tren -CH_2; etmalt -CH_2); 1.30 (t, 3H, etmalt -CH_3). Ratio of the Isomer A: Isomer B = 4: 3. IR (KBr)/cm^{-1}: 3421, 3285, 3120, 1602, 1551, 1264, 1192, 1097, 846, 625, 559. Anal. Required for $C_{13}H_{25}Cl_2CoN_4O_{11}$·EtOH: C, 30.57, H, 5.30, N, 9.51%. Found: C, 30.88, H, 5.51, N, 9.14%. MS (ESI, positive ion): *m/z* 304.0344 [Co^{II}(tren)]$(ClO_4)^+$ (simulated: 304.0343); 343.1176 [Co^{III}(tren)(etmalt)-H]$^+$ (simulated: 343.1175); 443.0741 [Co^{III}(tren)(etmalt)]$(ClO_4)^+$ (simulated: 443.0738).

[Co(tren)(dhp)]$(ClO_4)_2$ (**11**)

It was synthesized analogously to **9** using [Co(tren)Cl_2]Cl·H_2O (201 mg, 0.61 mmol), dhpH (90 mg, 0.65 mmol), KOH (1 M, 0.64 mL) and $NaClO_4$·H_2O (1.45 g, 10,36 mmol). The isolated purple microcrystalline crude product was recrystallized from acetonitrile and EtOH. Yield: 98 mg (30%). ^{1}H NMR of isomer A (400 MHz, D_2O): δ/ppm = 7.49 (d, 1H, dhp H); 6.67 (d, 1H, dhp H); 3.83 (s, 3H, dhp N-CH_3); 3.70 (m, 2H, tren -CH_2); 3.35 (m, 2H, tren -CH_2); 3.15 (m, 4H, tren -CH_2); 2.95 (m, 2H, tren -CH_2); 2.88 (m, 2H, tren -CH_2); 2.54 (s, 3H, dhp -CH_3). ^{1}H NMR of isomer B (400 MHz, D_2O): δ/ppm = 7.54 (d, 1H, dhp H); 6.77 (d, 1H, dhp H); 3.82 (s, 3H, dhp N-CH_3); 3.61 (m, 2H, tren -CH_2); 3.35 (m, 2H, tren -CH_2); 3.15 (m, 4H, tren -CH_2); 2.95 (m, 4H, tren -CH_2); 2.45 (s, 3H, dhp -CH_3). Ratio of the Isomer A: Isomer B = 2: 1. IR (KBr)/cm^{-1}: 3445, 3270, 3168, 1611, 1549, 1508, 1461, 1342, 1284, 1097, 918, 625. Anal. Required for $C_{13}H_{26}Cl_2CoN_5O_{10}$·0.5$H_2O$: C, 28.33, H, 4.94, N, 12.71%. Found: C, 27.98, H, 4.70, N, 12.49%. MS (ESI, positive ion): *m/z* 304.0342 [Co^{II}(tren)]$(ClO_4)^+$ (simulated: 304.0343); 342.1334 [Co^{III}(tren)(dhp)-H]$^+$ (simulated: 342.1335); 442.0895 [Co^{III}(tren)(dhp)]$(ClO_4)^+$ (simulated: 442.0898).

[Co(tpa)(etmalt)]$(ClO_4)_2$ (**12**)

To the purple-red solution of [Co(tpa)Cl_2]Cl (201 mg, 0.44 mmol) in 10 mL water were added etmaltH (61 mg, 0.44 mmol) and KOH (1 M, 0.44 mL). The mixture was kept at room temperature for overnight. The colour of the reaction mixture changed to red. Some purple solid appeared immediately after adding $NaClO_4$·H_2O (130 mg, 0.93 mmol). The mixture was standing at 4 °C for few hours; the solid appeared was filtered off and dried in vacuo. Yield: 111 mg (37%). ^{1}H NMR of isomer A (400 MHz, D_2O): δ/ppm = 9.28 (d, 1H, Ar-H tpa); 8.44 (d, 2H, Ar-H tpa); 8.24–6.67 (m, 11H, Ar-H tpa, etmalt H); 5.58 (m, 2H, tpa -CH_2); 5.17 (m, 2H, tpa -CH_2); 5.02 (d, 2H, tpa -CH_2); 2.73 (q, 2H, etmalt -CH_2); 0.97 (t, 3H, etmalt -CH_3). ^{1}H NMR of isomer B (400 MHz, D_2O): δ/ppm = 9.19 (d, 1H, Ar-H tpa); 8.57 (d, 2H, Ar-H tpa); 8.24–6.67 (m, 11H, Ar-H tpa, etmalt); 5.58 (m, 2H, tpa -CH_2); 5.17 (m, 4H, tpa -CH_2); 3.39 (q, 2H, etmalt -CH_2); 1.54 (t, 3H, etmalt -CH_3). Ratio of the Isomer A: Isomer B = 3: 2. IR (KBr)/cm^{-1}: 3600, 3525, 3082, 2981, 2323, 1610, 1596, 1547, 1474, 1457, 1293, 1278, 1263, 1190, 1163, 1092, 995. Anal. Required for $C_{25}H_{25}Cl_2CoN_4O_{11}$·0.5$H_2O$: C, 43.12, H, 3.76, N, 8.05%. Found: C, 42.88, H, 3.64, N, 8.10%. MS (ESI, positive ion): *m/z* 174.5427 [Co^{II}(tpa)]$^{2+}$ (simulated: 174.5426); 448.0343 [Co^{II}(tpa)]$(ClO_4)^+$ (simulated: 448.0343); 244.0623 [Co^{III}(tpa)(etmalt)]$^{2+}$ (simulated: 244.0624). On standing X-ray quality crystals appeared from the mother liquor.

[Co(tpa)(dhp)]$(ClO_4)_2$ (**13**)

This was synthesized as **12**, using [Co(tpa)Cl_2]Cl (201 mg, 0.44 mmol), dhpH (61 mg, 0.44 mmol), KOH (1 M, 0.44 mL), $NaClO_4$·H_2O (130 mg, 0.93 mmol). The product was isolated as a deep purple microcrystalline solid. Yield: 157 mg (52%). ^{1}H NMR of isomer A (400 MHz, D_2O): δ/ppm = 9.31 (d, 1H, Ar-H tpa); 8.53 (d, 2H, Ar-H tpa); 8.05–6.40 (m, 11H, Ar-H tpa, dhp H); 5.58 (d, 2H, tpa -CH_2); 5.14 (s, 2H, tpa -CH_2); 5.04 (d, 2H, tpa -CH_2); 3.72 (s, 3H, dhp N-CH_3); 2.26 (s, 3H, dhp -CH_3). ^{1}H NMR of isomer B (400 MHz, D_2O): δ/ppm = 9.13 (d, 1H, Ar-H tpa); 8.53 (d, 2H, Ar-H tpa); 8.05–6.40 (m, 11H, Ar-H tpa, dhp H); 5.52 (d, 2H, tpa -CH_2); 5.16 (s, 2H, tpa -CH_2); 5.11 (d, 2H, tpa -CH_2); 3.89 (s, 3H, dhp N-CH_3); 2.94 (s, 3H, dhp -CH_3). Ratio of the Isomer A: Isomer B = 3: 2. IR (KBr)/cm^{-1}: 3524, 3080, 2980, 1610, 1552, 1505, 1488, 1444, 1336, 1277, 1090, 820, 771, 623, 591. Anal. Required for $C_{25}H_{26}Cl_2CoN_5O_{10}$·0.5$H_2O$: C, 43.18, H, 3.91, N, 10.07%. Found: C, 43.16, H, 3.77, N, 10.12%. MS (ESI, positive ion): *m/z* 174.5424 [Co^{II}(tpa)]$^{2+}$ (simulated: 174.5426); 448.0341 [Co^{II}(tpa)]$(ClO_4)^+$ (simulated: 448.0343); 243.5705 [Co^{III}(tpa)(dhp)]$^{2+}$ (simulated: 243.5704).

[Co(tpa)(malt)]$(ClO_4)_2$ (**14**)

This was synthesized as **12**, using [Co(tpa)Cl_2]Cl (199 mg, 0.44 mmol), maltH (56 mg, 0.44 mmol), KOH (1 M, 0.44 mL), $NaClO_4$·H_2O (130 mg, 0.93 mmol). The product was isolated as a red microcrystalline solid. Yield: 75 mg (25%). ^{1}H NMR of isomer A (400 MHz, D_2O): δ/ppm = 9.27 (d, 1H, Ar-H tpa); 8.43 (d, 2H, Ar-H tpa); 8.22 (d, 1H, malt H); 8.20–7.20 (m, 10H, Ar-H tpa, malt H); 5.60 (m, 2H, tpa -CH_2); 5.17 (s, 2H, tpa -CH_2); 5.01 (d, 2H, tpa -CH_2); 2.31 (s, 3H, malt -CH_3). ^{1}H NMR of isomer B (400 MHz, D_2O): δ/ppm = = 9.21 (d, 1H, Ar-H tpa); 8.59 (d, 2H, Ar-H tpa); 8.20–7.20 (m, 10H, Ar-H tpa, malt H); 6.66 (d, 1H, malt); 5.60 (m, 2H, tpa -CH_2); 5.20 (s, 2H, tpa -CH_2); 5.12 (d, 2H, tpa -CH_2); 2.92 (s, 3H, malt -CH_3). Ratio of the Isomer A: Isomer B = 1: 1. IR (KBr)/cm^{-1}: 3600, 3535, 3080, 2981, 1610, 1549, 1474, 1458, 1446, 1360, 1274, 1212, 1162, 1092, 932, 849, 823, 772, 734, 623, 582, 446. Anal. Required for $C_{24}H_{23}Cl_2CoN_4O_{11}$·1.5$H_2O$: C, 41.16, H, 3.74, N, 8.00%. Found: C, 41.20, H, 3.65, N, 7.98%. MS (ESI, positive ion): *m/z* 174.5405 [Co^{II}(tpa)]$^{2+}$ (simulated: 174.5426); 237.0504 [Co^{III}(tpa)(malt)]$^{2+}$ (simulated: 237.0546).

2.3. NMR, IR and electrospray ionization mass spectrometric (ESI-MS) measurements

NMR measurements were carried out using a Bruker Avance I 400 MHz NMR spectrometer at 298 K, samples prepared in D_2O or d^6-DMSO.

Calibration was performed using the residual solvent signals (D_2O: 4.79 ppm; d^6-DMSO: 2.50 ppm). IR spectra as KBr pellets were recorded on a Perkin Elmer FTIR Paragon 1000 PC instrument at the Department of Organic Chemistry, University of Debrecen. High resolution ESI-TOF MS measurements in the positive mode were carried out on a Bruker maXis II UHR ESI-TOF MS instrument at the Department of Inorganic and Analytical Chemistry, University of Debrecen. The concentration of the samples was 10 μg/mL and the solvent was water or methanol. The instrument was equipped with an electrospray ion source, where the voltage was 4.5 kV. The drying gas was N_2. The flow rate was 4 l/min and the drying temperature was 200 °C. Na-formate was injected after each measurements enabling internal *m/z* calibration. The spectra were evaluated with Bruker Compass Data Analysis 4.4. software.

2.4. Crystal structure analysis

X-ray quality crystals were grown by slow evaporation of the appropriate mother liquors. A suitable crystal was fixed under microscope onto a Mitegen loop using high density oil. Diffraction intensity data collection was carried out using a Bruker-D8 Venture diffractometer equipped with INCOATEC IμS 3.0 dual (Cu and Mo) sealed tube micro sources and Photon II Charge-Integrating Pixel Array detector using Mo Kα (λ = 0.71073 Å) or Cu Kα (λ = 1.54178 Å) radiation. The structures were determined using room temperature data collection. High multiplicity data collection and integration was performed using the APEX3 (Ver. 2017.3–0, Bruker AXS Inc., 2017.) software. Data reduction and multi-scan absorption correction was performed using SAINT (Ver. 8.38A, Bruker AXS Inc., 2017). The structures could be solved using direct methods and refined on F2 using the SHELXL program [28] incorporated into APEX3 suite. Refinement was performed anisotropically for all non-hydrogen atoms. Hydrogen atoms were placed into geometric positions except N—H and O—H protons which were located on the difference electron density map and the N—H or O—H distances were constrained. The CIF file was merged and manually edited using the Publcif software [29]. Results of X-ray diffraction structure determinations were very good according to the Checkcif of PLATON software [30] and structural parameters such as bond length and angle data are in the expected range. The structures are also stabilized with weak C—H···O or C—H···N hydrogen bonds in several cases as well as strong hydrogen bonds with solvent water molecules. The crystallographic and refinement details can be seen in Table 1. CCDC contains the supplementary crystallographic data for **2**, **4**, **5**, **12** and [Co(en)$_2$(dhp)](ClO$_4$)$_2$ (**15**) with deposition numbers 2050296-2050300, respectively. These data can be obtained free of charge from The Cambridge Crystallographic Data Centre via www.ccdc.cam.ac.uk/data_request/cif.

2.5. Cyclic voltammetric (CV) studies

Cyclic voltammetric measurements were performed within the voltage range + 500 to −1200 mV, at room temperature in aqueous solution using a BASi Epsilon Eclipse instrument equipped with a three-electrode system, that consists of a Ag/AgCl/3 M KNO_3 reference electrode ($E_{1/2}$ = +209 mV vs. NHE), a platinum wire auxiliary electrode (ALS Co. Japan), and a glassy carbon (CHI104) working electrode. Aqueous solution of $K_3[Fe(CN)_6]$ was used to calibrate the system ($E_{1/2}$ = +458 mV vs. NHE in 0.50 M KCl) [31]. The samples were degassed before the measurements using argon gas. The concentration of the samples was 0.01 M and the potential sweep rates were 100 or 200 mVs^{-1} during the determination of the redox potentials. KNO_3 was used

Table 1
Crystallographic parameters and refinement details for complexes **2**, **4**, **5**, **12** and [Co(en)$_2$(dhp)](ClO$_4$)$_2$ (**15**).

Chemical formula	$C_{30}H_{21}CoN_4O_3{\cdot}2(ClO_4){\cdot}0.5(C_2H_6O){\cdot}1.5(H_2O)$ (**2**)	$C_{31}H_{24}CoN_5O_2{\cdot}2(ClO_4){\cdot}H_2O$ (**4**)	$C_{26}H_{21}CoN_4O_3{\cdot}2(ClO_4)$ (**5**)	$C_{25}H_{25}CoN_4O_3{\cdot}2(ClO_4){\cdot}H_2O$ (**12**)	$C_{11}H_{24}CoN_5O_2{\cdot}2(ClO_4)$ (**15**)
M_r	793.39	774.40	695.30	705.34	516.18
Crystal system, space group	Monoclinic, *C*2/*c*	Triclinic, $P\bar{1}$	Monoclinic, *Cc*	Orthorhombic, $Pna2_1$	Monoclinic, $P12_1/m1$
Temperature (K)	296	299	293	299	293
a, *b*, *c* (Å)	33.7250 (9), 10.7919 (3), 22.2809 (6)	11.052 (3), 11.664 (4), 14.589 (4)	21.884 (3), 10.3975 (16), 15.216 (3)	16.9181 (6), 19.4673 (7), 8.7496 (3)	7.2494 (3), 35.3412 (16), 7.8650 (4)
α, β, γ (°)	90, 119.767 (1), 90	82.546 (9), 73.346 (8), 62.708 (8)	90,126.052 (6), 90	90, 90, 90	90, 103.825 (2), 90
V (Å^3)	7039.3 (3)	1601.2 (8)	2799.2 (8)	2881.68 (18)	1956.66 (16)
Z	8	2	4	4	4
Radiation type	Cu *K*α	Mo *K*α	Mo *K*α	Cu *K*α	Mo *K*α
μ (mm^{-1})	5.83	0.77	0.87	7.01	1.21
Crystal size (mm)	0.19 × 0.17 × 0.10	0.37 × 0.16 × 0.05	0.36 × 0.18 × 0.12	0.16 × 0.14 × 0.12	0.75 × 0.37 × 0.13
Diffractometer	Bruker D8 VENTURE				
Absorption correction	Multi-scan *SADABS2016*/2 - Bruker AXS area detector scaling and absorption correction				
T_{min}, T_{max}	0.59, 0.75	0.66, 0.96	0.82, 0.90	0.41, 0.49	0.53, 0.86
No. of measured, independent and observed [$I > 2\sigma(I)$] reflections	57515, 6460, 5265	33585, 6378, 4307	24915, 5308, 4481	17652, 5041, 4436	28065, 3777, 3502
R_{int}	0.065	0.100	0.036	0.045	0.060
(sin θ/λ)$_{max}$ (Å^{-1})	0.605	0.621	0.610	0.595	0.610
$R[F^2 > 2\sigma(F^2)]$, $wR(F^2)$, *S*	0.086, 0.240, 1.43	0.081, 0.238, 1.05	0.055, 0.158, 1.01	0.043, 0.119, 1.01	0.076, 0.210, 1.15
No. of reflections	6460	6378	5308	5041	3777
No. of parameters	496	459	399	406	298
No. of restraints	10	2	2	4	8
H-atom treatment	H atoms treated by a mixture of independent and constrained refinement	H atoms treated by a mixture of independent and constrained refinement	H-atom parameters constrained	H atoms treated by a mixture of independent and constrained refinement	H atoms treated by a mixture of independent and constrained refinement
$(\Delta/\sigma)_{max}$	0.039	0.001	0.006	< 0.001	< 0.001
$\Delta\rangle_{max}$, $\Delta\rangle_{min}$ (e Å^{-3})	0.89, −0.38	0.90, −0.46	0.46, −0.54	0.51, −0.34	2.48, −0.72
Absolute structure	–	–	Refined as an inversion twin.	Refined as an inversion twin.	–
Absolute structure parameter	–	–	0.49 (4)	0.395 (6)	–

as supporting electrolyte with the concentration of 0.20 M.

2.6. Biological studies

2.6.1. Cell culture

HeLa human cervical cancer cells were purchased from the European Collection of Cell Cultures (ECACC) and cultured according to the supplier's recommendations at 37 °C in a humidified atmosphere of 5% CO_2 and 95% air.

2.6.2. MTT assay

MTT assay was used to determine the toxicity of selected complexes, **2**, **4**, **5**, **7**, **11**, **13**, $[Co(bipy)_2Cl_2]Cl$, $[Co(phen)_2Cl_2]Cl$ and cisplatin. HeLa cells were seeded in 96-well tissue culture plates at a density of 5000 cells/well, incubated for 24 h and then serum-starved in 1% foetal bovine serum (FBS)-containing media overnight. On the day of treatment, various concentrations of the title compounds were added and incubated for 72 h (total volume 100 μL). Stock solutions of the compounds were prepared at a concentration of 1 mM in MEM and diluted necessarily. After 72 h, 10 μL of a 5 mg/mL solution of MTT in PBS was added to each well and the plate was incubated for an additional 1.5 h. The MEM/MTT mixture was aspirated and 100 μL of DMSO was added to dissolve the resulting formazan crystals produced by cell metabolism. The absorbance was measured at 540 nm using a Thermo Scientific Multiscan Go spectrophotometer. Absorbance values were normalized to DMSO-containing control wells and plotted as concentration of complex versus % cell viability. IC_{50} values were calculated from the resulting dose dependent curves using GraphPad Prism 8.0.1 software. The reported IC_{50} values are the average of at least three independent experiments, each contained four replicates per concentration level.

3. Results and discussion

3.1. Synthesis and characterization

For the synthesis of the novel mixed ligand cobalt(III) complexes **1–14** the appropriate $[Co(2N)_2Cl_2]Cl$ type or $[Co(4N)Cl_2]Cl$ chloride precursors (2N = phen, bipy, ampy or en; 4N = tren or tpa) were prepared using published procedures [19,25–27]. In the case of the former set of species both *cis* and *trans* isomers can exist depending upon the position of the chloride ligands. In solution, these isomeric forms are in equilibrium and due to the complexation with the (2O) ligands the equilibrium can be shifted to the direction of the formation of the product via rearrangement of the (2N) coordinating ligands. Although in many cases the *trans* isomer of the $[Co(2N)_2Cl_2]Cl$ precursors also appeared as minor impurity in the crude $[Co(2N)_2(2O)]X_n$ products via optimization of the reaction conditions the pure complexes could be obtained. For the synthesis of the complexes **1–14** with the general formulae of $[Co(4N)(2O)]X_n$ or $[Co(2N)_2(2O)]X_n$ maltH, etmaltH or dhpH as (2O) donor ligands were used. In order to facilitate the deprotonation and coordination of the (2O) ligand the precursor chlorido complexes and the appropriate (2O) derivatives were reacted in equimolar ratio in the presence of one equivalent base (KOH, NaOH or Et_3N). The changing colour of the solution over time has indicated the complexation. The final products were isolated as the perchlorate salts since the large sized ClO_4^- turned to be the best counter ion to facilitate the formation of pure complexes from the reaction mixture. For **4** and **7** green while in the other cases red/purple crystals appeared. All the complexes are air stable, soluble in polar solvents (DMSO, MeOH) and slightly soluble in water.

Identity and purity of the complexes **1–14** were first checked using ^1H NMR. Based on the structure of the products two types of isomers can be expected for them depending upon the presence of either a 4N or a 2N donor chelator. Due to the coordination of the 4N donor ligands the formation of two asymmetric geometric isomers while in the case of two symmetrical 2N donors two optical isomers can be assumed [13]. However, for the asymmetrical 2N donor, ampy, in principle four geometrical isomers are possible. As a result, duplication of the signals was noticed in the spectra of the tren and tpa containing products (Fig. 2, Figs. S1–S5) while this was not the case for the $[Co(2N)_2(2O)]X_n$ type complexes (Fig. 3, Figs. S6–S12). Assignation of the NMR signals is demonstrated on two representative examples, **9** and **5**.

In the spectrum of $[Co(tren)(malt)](ClO_4)_2$ (**9**) the $-CH_2$ signals of tren (3.8–2.8 ppm) and the signals belonging to the two ring protons of malt are well separated (Fig. 2). In the low field region of the spectrum four doublets appear, two around 8.15 ppm that can be assigned to the *36* proton owing to the electron withdrawing character of the ring oxygen while the two doublets at 6.95 ppm belong to the *35* proton. Duplication of these low field signals clearly indicates the presence of two geometric isomers in the inert **9**. The presence of two singlets for the $-CH_3$ group (*37*) supports the same. The integral values in all signal pairs indicate a ratio of isomer A to isomer B ~ 6.7:1 for **9**.

Assignation of the NMR signals was more difficult for the analogous tpa complexes due to the presence of three pyridyl arms of the 4N donor ligand beside the low field resonances of the various 2O ligands therefore COSY measurements were also carried out (Fig. S13). Analysis of the spectra revealed that all of these type of complexes (**9–14**) were also obtained as a mixture of two isomers; for the ratios see the Experimental section.

As far as the NMR spectrum of $[Co(bipy)_2malt](ClO_4)_2$ (**5**) is concerned (Fig. 3), only one singlet can be detected in the aliphatic region obviously belonging to the $-CH_3$ group of malt. Unlike for **9**, lack of duplication of the resonances is in line with the possibility of the formation of stereoisomers only for **5**. The aromatic region of **5** is more complex (Fig. 3) compared to that of **9**. In this region of the COSY spectrum of **5** three spin systems can be identified and marked by solid, dotted and dashed lines, respectively, belonging to the malt, py-1 and py-2 ring protons. Fig. 3 also reveals that due to the slightly different shielding of the neighbouring chemical environment the signals of the appropriate py-1 and py-2 protons for the two coordinating bipy ligands resonate at slightly different frequencies. As Fig. 3 indicates, the highest chemical shift (9.03 ppm) belongs to the *2* and *12* protons due to the close vicinity of the ring nitrogen of bipy and the malt oxygens both with electron withdrawing character. Since the *9* and *19* protons are further apart from the malt oxygens they resonate at 8.94–8.89 ppm. The two malt protons *36* (8.47 ppm) and *35* (7.12 ppm) give the expected doublets in the spectrum. For the complete assignation, see Fig. 3.

High resolution electrospray ionization mass spectrometry (ESI-MS) also proved the supposed composition of the complexes. The $[M]^{2+}$ ions (M = [Co(4N)(2O)] or $[Co(2N)_2(2O)]$) were identified in the spectra of **1–7**, **12–14**; $[M + ClO_4]^+$ in the spectra of **8–11**; $[M\text{-}H]^+$ in the spectra of **9**, **10**, **11**. In agreement with the previously reported results [32] reduction of Co(III) to Co(II) in the complexes was detectable under mass spectrometric conditions. For instance in the case of **4**, **5**, **6** and **7** $[Co^{II}(2N)_2]^{2+}$; for **12**, **13** and **14** $[Co^{II}(4N)]^{2+}$ while for **9–13** $[Co^{II}(4N)ClO_4]^+$ ions were detected. The corresponding measured and calculated isotope patterns were in good agreement as it is demonstrated on some representative examples in Figs. S14–S27.

The identity and purity of the complexes was further proved by the elemental analysis data. The results revealed that the complexes contain water (ethanol for **10**) in their crystal lattice with the exception of **1**, **5**, **8** and **9**.

In the case of **4**, **5**, **12** slow evaporation of the aqueous while for **2** the ethanolic solution of the complexes resulted in the formation of single crystals suitable for X-ray diffraction studies. Although every our efforts to obtain pure $[Co(en)_2(dhp)](ClO_4)_2$ (**15**) were failed from one of the aqueous solutions during recrystallization trials single crystals of the title compound also appeared and therefore this complex was also involved in the X-ray studies. The determined crystal structures together with key bond length and angle values are shown in Figs. 4–6 and Figs. S28–29 while the crystallographic parameters and refinement details are summarized in Table 1. Structures of the complexes show the expected

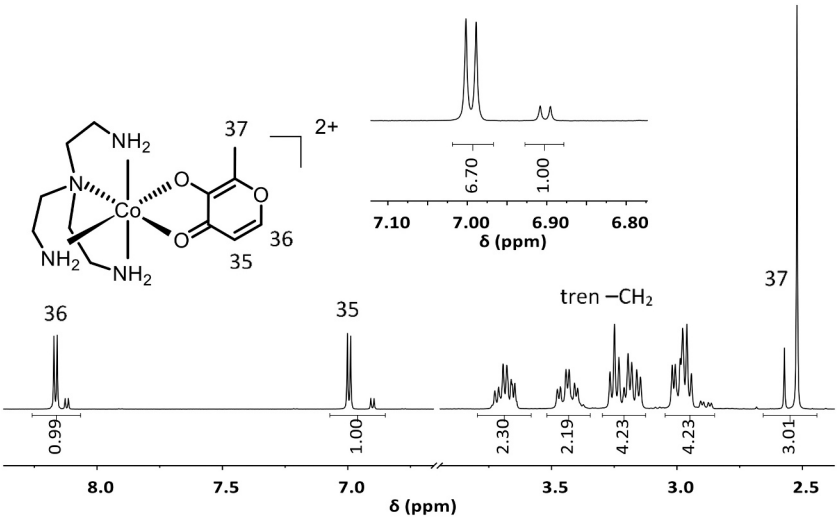

Fig. 2. ^{1}H NMR spectrum of [Co(tren)malt]$(ClO_4)_2$ (**9**) in D_2O. Inlet indicates the ratio of the two geometric isomers.

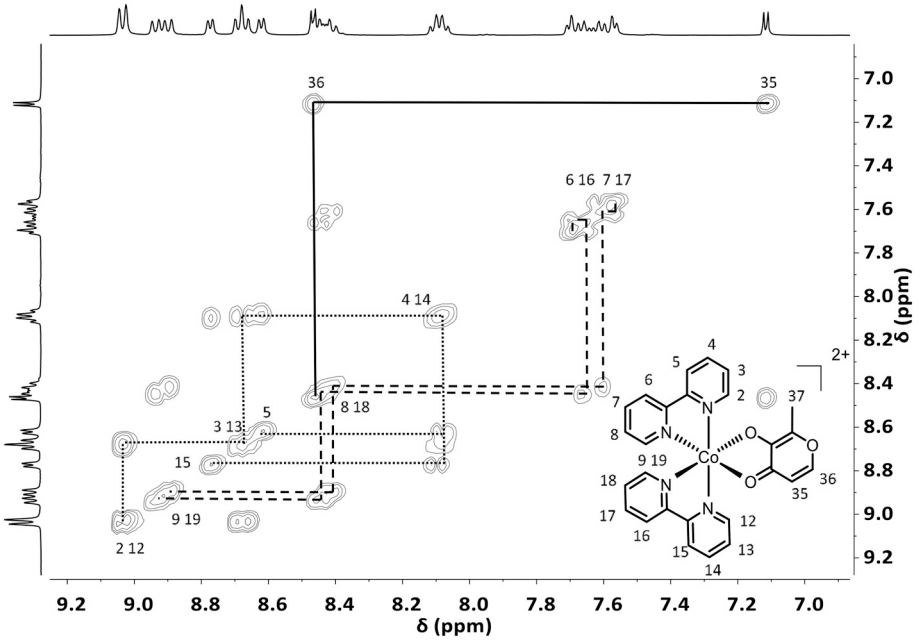

Fig. 3. The low field region of the COSY spectrum of [Co(bipy)$_2$malt]$(ClO_4)_2$ (**5**) in d^6-DMSO.

octahedral geometry with one coordinating malt (or etmalt, dhp) via the carbonyl and the hydroxyl O donor atoms beside the 4N or the two 2N donor other ligands. The corresponding bond length (C═O···M = 1.89–1.91 Å; C—O···M = 1.87–1.91 Å) and angle values related to analoguous complexes (C═O···M = 2.14 [15] Å; C—O···M = 2.02 [17] Å) in Cambridge Structural Database (Version 5.41, Update August, 2020) reveal that the appropriate data obtained in this work fall into the low range typical for octahedral complexes with similar ligands. Based on the determined absolute configurations out of the $[Co(2N)_2(2O)]^{2+}$ complexes, **4**, **15** are Δ while **2**, **5** are Λ optical isomers. **12** was crystallized as the *trans* isomer since the tertiary amine of the 4N ligand was observed to be *trans* to the deprotonated hydroxyl group of the etmalt ligand.

3.2. Electrochemical studies

Electrochemical behaviour of the studied complexes was explored under the conditions given in Section 2.5. Cathodic peaks with the appropriate potentials (E_{pc}) in all cyclic voltammograms (CVs) were observable indicating clearly the reduction of the complexes (Fig. 7; Figs. S30–31), while anodic peaks (with E_{pa}) were not always detectable (see the measured E_{pc} and E_{pa} values in Table 2). These redox processes must belong to the reduction of Co(III) to Co(II) because maltH and its derivatives (etmaltH, dhpH) did not show redox activity under the same conditions. In addition, the precursor chlorido complexes ([Co(2N)$_2$Cl$_2$]Cl; [Co(4N)Cl$_2$]Cl) have also been studied but the CV peak(s) characteristic for their redox reaction(s) appeared at different potentials, see Table 2.

Although for well-established inferences more data would be desirable, based on the redox potential values presented in Table 2 the following conclusions can be drawn: i) comparison of the E_{pc} values for a given 2O ligand (e.g. malt) containing complexes with different 4N or 2x2N donor ligand(s) in the coordination sphere of the metal ion the difference of the stability of the corresponding Co(III) and Co(II) complexes after cathodic reduction (Δlogβ) increases in the direction of phen < bipy < tpa < ampy < en < tren resulting in least reducible Co(III)

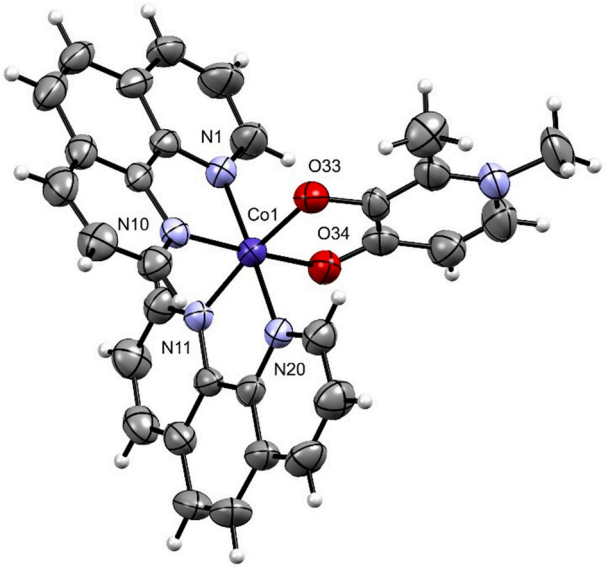

Fig. 4. Ortep view of Δ-[Co(phen)$_2$(dhp)]$^{2+}$ (**4**) at 50% probability level. The perchlorate counter ions and solvent molecules are not shown for clarity. Key bond lengths [Å] and angles [°] are Co1-O33 1.867(4), Co1-O34 1.897(4), Co1-N1 1.939(4), Co1-N10 1.948(4), Co1-N11 1.943(5), Co1-N20 1.932(4); O33-Co1-O34 88.19(19), O33-Co1-N10 92.72(18), O34-Co1-N11 87.14(18), N20-Co1-N10 93.57(18).

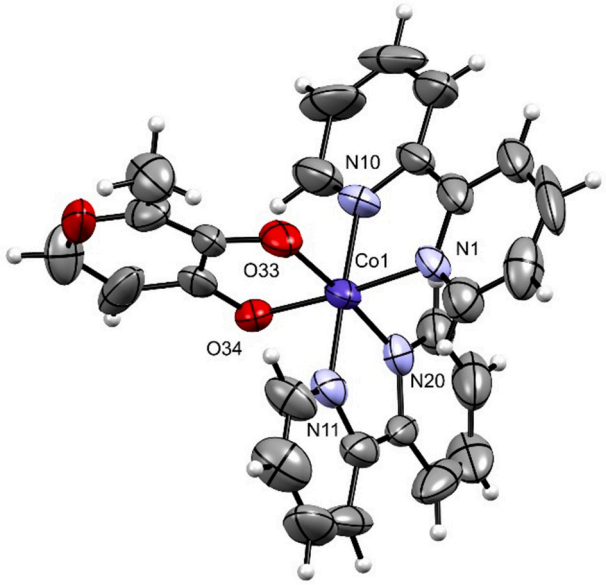

Fig. 5. Ortep view of Λ-[Co(bipy)$_2$(malt)]$^{2+}$ (**5**) at 50% probability level. The perchlorate counter ions are not shown for clarity. Key bond lengths [Å] and angles [°]: Co1-O33 1.906(7), Co1-O34 1.885(7), Co1-N1 1.950(8), Co1-N10 1.921(10), Co1-N11 1.916(11), Co1-N20 1.895(10) O33-Co1-O34 87.35(18), O33-Co1-N10 88.5(4), O34-Co1-N11 88.0(3), N20-Co1-N10 94.8(4).

complexes with decreasing E_{pc} values (Fig. 7). This trend can be rationalized by the back coordination capability of the aromatic N-donor atoms, in general, stabilizing therefore the lower oxidation state Co(II) form more than in the case of the complexes with aliphatic N donor ligands. ii) Both for the tripodal ligands, tpa and tren, capable of forming fused chelates the increased stability of the Co(III) species over the corresponding 2x2N containing ones (phen and bipy or en, respectively) can be detected via the increased Δlogβ values. iii) When the effects of the presence of the different coordinating 2O ligands are compared for a

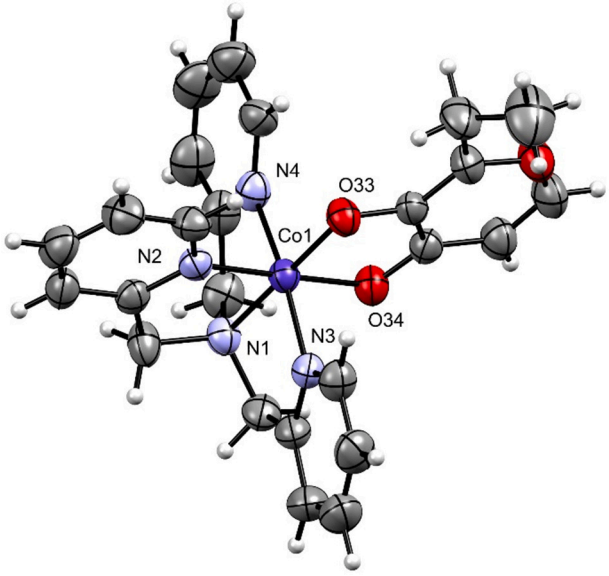

Fig. 6. Ortep view of *trans*-Co(tpa)(etmalt)]$^{2+}$ (**12**) at 50% probability level. The perchlorate counter ions and solvent molecules are not shown for clarity. Key bond lengths [Å] and angles [°]: Co1-O33 1.874(3), Co1-O34 1.910(4), Co1-N1 1.936(4), Co1-N2 1.904(4), Co1-N3 1.917(5), Co1-N4 1.929(5) O33-Co1-O34 87.71(15), O33-Co1-N3 95.4(2), O34-Co1-N3 89.99(18), O34-Co1-N4 88.34(19).

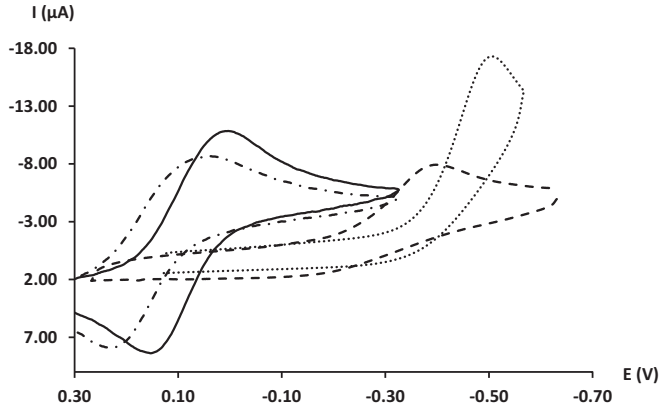

Fig. 7. Cyclic voltammograms of selected malt complexes, **1** (dotted), **2** (dashdotted), **5** (solid), **8** (dashed) in H_2O ($c_{complex}$ ~ 0.01 M, I = 0.20 M (KNO_3), v = 200 mV/s).

given 4N or 2x2N containing complex the Δlogβ of the corresponding Co (III) and Co(II) species increases as follows: malt ~ etmalt << dhp. This can be interpreted with increasing pK_a values of the ligands (8.44, 8.49 and 9.78 for maltH, etmaltH and dhpH, respectively) and the more delocalised electronic structure of the dhp anion. iv) The effect of the various 2O donor ligands (malt vs. dhp) is larger on the E_{pc} values in complexes with 2x2N ligands over the ones with 4N ligands. v) For the phen and bipy complexes with the largest E_{pc} values (smallest Δlogβ values) the reduction is reversible indicating the relative stability of the Co(II) species formed preventing it from immediate dissociation.

The results of the CV study reveal that in each case a 4N → 2x2N replacement in the Co(III) complexes results in increase in the E_{pc} values making the 2x2N type complexes more reducible than those with identical type (aromatic or aliphatic) 4N donor ligand. This allows the synthesis of candidates with tailored redox features suitable for selective reduction under hypoxic conditions.

Table 2
Measured cathodic (E_{pc}) and anodic (E_{pa}) peak potential values (mV) of the Co(III) complexes referenced to Ag/AgCl and the calculated values against NHE.

Complex	#	E_{pc} [mV] vs. Ag/AgCl	E_{pa}	E_{pc} [mV] vs. H_2/H^+	E_{pa}
$[Co(en)_2Cl_2]Cl$		−367	–	−158	–
$[Co(en)_2(malt)](ClO_4)_2$	**1**	−504	–	−295	–
$[Co(phen)_2Cl_2]Cl$		90	177	299	386
$[Co(phen)_2(malt)](ClO_4)_2$	**2**	41	228	250	437
$[Co(phen)_2(etmalt)](ClO_4)_2$	**3**	44	228	253	437
$[Co(phen)_2(dhp)](ClO_4)_2$	**4**	−168	–	41	–
$[Co(bipy)_2Cl_2]Cl$		142	240	351	449
$[Co(bipy)_2(malt)](ClO_4)_2$	**5**	3	149	212	358
$[Co(bipy)_2(etmalt)](ClO_4)_2$	**6**	14	143	223	352
$[Co(bipy)_2(dhp)](ClO_4)_2$	**7**	−163	–	46	–
$[Co(ampy)_2Cl_2]Cl$		−108	–	101	–
$[Co(ampy)_2(malt)](ClO_4)_2$	**8**	−333	–	−124	–
$[Co(tren)(malt)](ClO_4)_2$	**9**	−579	–	−370	–
$[Co(tren)(etmalt)](ClO_4)_2$	**10**	−592	–	−383	–
$[Co(tren)(dhp)](ClO_4)_2$	**11**	−682	–	−473	–
$[Co(tpa)(etmalt)](ClO_4)_2$	**12**	−358	–	−149	–
$[Co(tpa)(dhp)](ClO_4)_2$	**13**	−459	–	−250	–
$[Co(tpa)(malt)](ClO_4)_2$	**14**	−317	–	−108	–

3.3. Stability, lipophilicity and biological studies

Prior screening the antiproliferative activity of the complexes, their aqueous stability and lipophilic/hydrophilic character were also studied. Aqueous stability of the dissolved complexes in D_2O (for **4** also in PBS) was explored using NMR for 72 h at room temperature. As representative examples, time-dependent NMR spectra are shown in Figs. S32–38 and reveal that the complexes in this study exhibit no measurable change indicating high kinetic inertness.

Distribution coefficients (log P) of compounds **2**, **4**, **5**, **7**, **11**, **13** were determined by shake-flask method in *n*-octanol/water at 25 °C using a concentration of ~2 mM to assess their lipophilicity and ability to cross biological membranes by passive diffusion. The obtained log *P* values of the studied complexes (<−2.5) support the highly hydrophilic character of these complexes most likely due to their positive charge formed upon dissolution in water followed by dissociation of the non-coordinating perchlorate counter ion. This may indicate that the differences in the cytotoxic character of these selected complexes (vide infra) are probably not related to their significantly different lipophilic/hydrophilic character.

Among the novel cobalt(III) complexes **2**, **4**, **5**, **7**, **11** and **13** were selected for biological screening against human cervical carcinoma, HeLa, cells. Details of the assay are outlined in Section 2.6. Results, as the calculated IC_{50} values are summarized in Table 3 while cell viability profiles are shown in Figs. S39–40. The presented data in Table 3 reveal that the tren and tpa containing dhp complexes did not show antiproliferative activity in the measured concentration range. This can be rationalized by the very negative E_{pc} values of these complexes making them the least reducible ones among the selected compounds. However, if the 4N donor tripodal amine is replaced by two 2N donors they become active. The activity of **5** and **7** having the malt or dhp ligands, respectively, increased considerably compared to that of $[Co(bipy)_2Cl_2]Cl$. Moreover, **7** had lower IC_{50} value than **5** suggesting a positive effect of dhp; may be due to its better Fe(III) binding capability. This difference in favour of dhp over malt is disappeared when the activity of **2** and **4** are compared and can be rationalized by the effect of the presence of the phen ligands in both complexes contributing mostly to the biological action. This assumption is also supported by the high activity of $[Co(phen)_2Cl_2]Cl$ having none of the above 2O ligands. Notably, complexes **2**, **4** and **7** are more active than the clinically used cisplatin or carboplatin against this cancer cell line.

Table 3
IC_{50} values of selected complexes (**2**, **4**, **5**, **7**, **11**, **13**), $[Co(bipy)_2Cl_2]Cl$, $[Co(phen)_2Cl_2]Cl$ and cisplatin against HeLa cells after 72 h incubation at 37 °C by MTT assay. Data represent a mean ± SD from at least three independent experiments, each of them made in four.

Compound	#	HeLa IC_{50} [μM]
$[Co(tren)(dhp)](ClO_4)_2$	**11**	>200
$[Co(tpa)(dhp)](ClO_4)_2$	**13**	>200
$[Co(bipy)_2Cl_2]Cl$		37.1 ± 2.3
$[Co(bipy)_2(malt)](ClO_4)_2$	**5**	23.3 ± 2.1
$[Co(bipy)_2(dhp)](ClO_4)_2$	**7**	9.7 ± 1.2
$[Co(phen)_2Cl_2]Cl$		4.4 ± 1.5
$[Co(phen)_2(malt)](ClO_4)_2$	**2**	3.8 ± 1.2
$[Co(phen)_2(dhp)](ClO_4)_2$	**4**	3.4 ± 1.2
Cisplatin		16.3 ± 1.2
Carboplatin[a]		46
maltH[b]		74

[a] From Ref. [33].
[b] From Ref. [34].

4. Conclusion

The district differences in the stability and in the rate of the ligand exchange reactions of Co(III) and Co(II) complexes with identical ligands make the Co(III) counterparts promising candidates as hypoxia-activated prodrugs carrying antitumor molecules. Previous studies revealed that a 4N + 2O donor atom environment results typically in reduction potential values of these Co(III) complexes falling into the desired −400 to −200 mV (vs. H_2/H^+) range determined by biological reductants. However, in some cases these types of complexes exhibited too negative E_{pc} values that might be shifted towards the proper range by the structural modification of these 4N + 2O type complexes. The aim of this study, therefore, was to explore the effect of the replacement of the most frequently applied tetradentate tripodal 4N donors by two chelating 2N donor ligands on the redox properties of $[Co(2N)_2(2O)]^{2+}$ type ternary complexes. DhpH and derivatives as 2O ligands were selected hoping to have an additional anticancer effect of the complexes due to their iron sequestering capability or due to the easy modification of the 2O ligand to construct heterobimetallic complexes [22].

In summary, replacement of the 4N donor ligands, tren or tpa, by two 4N donor ligands resulted in the decrease of the cathodic peak potential of the complexes indicating easier reduction and allowing therefore the tailoring of the redox properties of the complexes. Screening the selected compounds against a human derived cancer cell line, HeLa, revealed that, i) unlike the $[Co(2N)(2O)]X_2$ derivatives, the complexes containing 2N = bipy or phen ligands are active. Assuming similar uptake by the cells based on the rather hydrophilic character of all these complexes this difference can either be explained by the fact that the 4N donor ligand containing complexes can easier be reduced due to their more positive E_{pc} values but most likely by the fact that bipy and phen exhibit cytotoxicity on their own too. ii) While for 2N = bipy the presence of the 2O donor ligands results in significant activity increase compared to the chloride precursor, with 2N = phen all the complexes show comparable activities to each other that are all higher than with bipy. iii) All the selected $[Co(2N)_2(2O)]^{2+}$ complexes have better anticancer activity than cisplatin or carboplatin against the screened HeLa cell line.

CRediT authorship contribution statement

Sándor Nagy: Investigation, Writing - original draft. **Emese Tóth**: Investigation. **István Kacsir**: Investigation. **Attila Csaba Bényei**: Investigation. **Péter Buglyó**: Conceptualization, Methology, Supervision, Writing review & editing.

Declaration of Competing Interest

The authors declare that they have no known competing financial

interests or personal relationships that could have appeared to influence the work reported in this paper.

Acknowledgements

The authors would like to say sincere thanks to Prof. Ferenc Erdődi (Department of Medical Chemistry, University of Debrecen) for providing the facilities for the anti-proliferative study. The research was supported by the EU and co-financed by the European Regional Development Fund under the project GINOP-2.3.2-15-2016-00008.

Appendix A. Supplementary data

Supplementary data to this article can be found online at https://doi.org/10.1016/j.jinorgbio.2021.111372.

References

[1] T.W. Failes, T.W. Hambley, Dalton Trans. (2006) 1895–1901.
[2] T.W. Failes, C. Cullinane, C.I. Diakos, N. Yamamoto, J.G. Lyons, T.W. Hambley, Chem. Eur. J. 13 (2007) 2974–2982.
[3] M.D. Hall, T.W. Failes, N. Yamamoto, T.W. Hambley, Dalton Trans. (2007) 3983–3990.
[4] P.J. Kim, R. Hocking, J.K. Clegg, P. Turner, S.M. Neville, T.W. Hambley, Dalton Trans. 41 (2012) 11293–11304.
[5] M.C. Heffern, N. Yamamoto, R.J. Holbrook, A.L. Eckermann, T.J. Meade, Curr. Opin. Chem. Biol. 17 (2013) 189–196.
[6] G. Wang, T.K. Hazra, S. Mitra, H.-M. Lee, E.W. Englander, Nucleic Acids Res. 28 (2000) 2135.
[7] Y. He, X. Gan, L. Zhang, B. Liu, Z. Zhu, T. Li, J. Zhu, J. Chen, H. Yu, Cell. Physiol. (2018) C389–C397.
[8] D.C. Ware, B.D. Palmer, W.R. Wilson, W.A. Denny, J. Med. Chem. 36 (1993) 1839–1846.
[9] V. Mallikarjun, D.J. Clarke, C.J. Cambell, Free Radic. Biol. Med. 53 (2012) 280–288.
[10] J. Jiang, C. Auchinvole, K. Fischer, C.J. Cambell, Nanoscale 6 (2014) 12104–12110.
[11] B.P. Green, A.K. Renfrew, A. Glenister, P. Turner, T.W. Hambley, Dalton Trans. 46 (2017) 15897–15907.
[12] M. Kozsup, E. Farkas, A.C. Bényei, J. Kasparkova, H. Crlikova, V. Brabec, P. Buglyó, J. Inorg. Biochem. 193 (2019) 94–105.
[13] P. Buglyó, I. Kacsir, M. Kozsup, I. Nagy, S. Nagy, A.C. Bényei, É. Kovats, E. Farkas, Inorg. Chim. Acta 472 (2018) 234–242.
[14] P.M. Jaffray, L.F. McClintock, K.E. Baxter, A.G. Blackman, Inorg. Chem. 44 (2005) 4215–4225.
[15] M. Piti, A. Croisy, D. Carrez, C. Boldron, B. Meunier, ChemBioChem 6 (2005) 686–691.
[16] C. Deegan, M. McCann, M. Devereux, B. Coyle, D.A. Egan, Cancer Lett. 247 (2007) 224–233.
[17] M. McCann, A.L.S. Santos, B.A. da Silva, M.T.V. Romanos, A.S. Pyrrho, M. Devereux, K. Kavanagh, I. Fichtnerg, A. Kelletth, Toxicol. Res. 1 (2012) 47–54.
[18] Y. Kato, T. Yamashita, M. Ishikawa, Oncol. Rep. 9 (2002) 565–569.
[19] S. Ghosh, A.C. Barve, A.A. Kumbhar, A.S. Kumbhar, V.G. Puranik, P.A. Datar, U. B. Sonawane, R.R. Joshi, J. Inorg. Biochem. 100 (2006) 331–343.
[20] D.O. Abe, A. Eskandari, K. Suntharalingam, Dalton Trans. 47 (2018) 13761–13765.
[21] E. Yasumoto, K. Nakano, T. Nakayachi, S.R.M.D. Morshedi, K. Hashomoto, H. Kikuchi, H. Nishikawa, M. Kawase, H. Sakagami, Anticancer Res. 24 (2004) 755–762.
[22] A. Ozsváth, R. Diószegi, A.C. Bényei, P. Buglyó, Dalton Trans. 49 (2020) 9254–9267.
[23] Z. Tyeklar, R.R. Jacobson, N. Wei, N.N. Murthy, J. Zubieta, K.D. Karlin, J. Am. Chem. Soc. 115 (1993) 2611–2689.
[24] P. Buglyó, T. Kiss, E. Kiss, D. Sanna, E. Garribba, G. Micera, J. Chem. Soc. Dalton Trans. (2002) 2275–2282.
[25] E. Kimura, S. Young, J.P. Collman, Inorg. Chem. 9 (1970) 1183–1191.
[26] W.C. Fernelius, Inorg. Synth. 2 (1946) 222–224.
[27] D.J. Ayeres, D.A. House, W.T. Robinson, Inorg. Chim. Acta 277 (1998) 234–242.
[28] G.M. Seldrick, Acta Cryst A64 (2008) 112–122.
[29] S.P. Westrip, J. Appl. Crystallogr. 43 (2010) 920–925.
[30] A.L. Spek, J. Appl. Crystallogr. 36 (2003) 7–13.
[31] E. Farkas, P. Buglyó, É.A. Enyedy, M.A. Santos, Inorg. Chim. Acta 357 (2004) 2451–2461.
[32] M. Kozsup, O. Dömötör, S. Nagy, E. Farkas, É.A. Enyedy, P. Buglyó, J. Inorg. Biochem. 204 (2020) 110963.
[33] H. Crlikova, H. Kostrhunova, J. Pracharova, M. Kozsup, P. Nagy, P. Buglyó, V. Brabec, J. Kasparkova, J. Biol. Inorg. Chem. 25 (2020) 339–350.
[34] A. Notaro, M. Jakubaszek, S. Koch, R. Rubbiani, O. Dömötör, É.A. Enyedy, M. Dotou, F. Bedioui, M. Tharaud, B. Goud, S. Ferrari, E. Alessio, G. Gasser, Chem. Eur. J. 26 (2020) 4997–5009.